



**HAL**  
open science

## **Pb<sup>2+</sup> potentiometric chemical sensors based on lead and silver doped thioarsenate glasses**

B. Alrifai, M. Kassem, J. Toufaily, Maria Bokova, Eugène Bychkov

### ► **To cite this version:**

B. Alrifai, M. Kassem, J. Toufaily, Maria Bokova, Eugène Bychkov. Pb<sup>2+</sup> potentiometric chemical sensors based on lead and silver doped thioarsenate glasses. *Solid State Sciences*, 2022, 131, pp.106955. 10.1016/j.solidstatesciences.2022.106955 . hal-04289934

**HAL Id: hal-04289934**

**<https://ulco.hal.science/hal-04289934>**

Submitted on 22 Nov 2023

**HAL** is a multi-disciplinary open access archive for the deposit and dissemination of scientific research documents, whether they are published or not. The documents may come from teaching and research institutions in France or abroad, or from public or private research centers.

L'archive ouverte pluridisciplinaire **HAL**, est destinée au dépôt et à la diffusion de documents scientifiques de niveau recherche, publiés ou non, émanant des établissements d'enseignement et de recherche français ou étrangers, des laboratoires publics ou privés.

## **Pb<sup>2+</sup> potentiometric chemical sensors based on lead and silver doped thioarsenate glasses**

B. Alrifai,<sup>1,2</sup> M. Kassem,<sup>\*1</sup> J. Toufaily,<sup>2</sup> M. Bokova,<sup>1</sup> and E. Bychkov<sup>1</sup>

<sup>1</sup>Université du Littoral Côte d'Opale (ULCO), LPCA, EA 4493, F-59140 Dunkerque, France

<sup>2</sup>MCEMA and LEADDER laboratories, Faculty of Sciences and EDST, Lebanese University, Hariri Campus, Beirut, Lebanon

\* Corresponding author. Université du Littoral Côte d'Opale, LPCA, 189A avenue M. Schumann, 59140 Dunkerque, France. Tel.: +33 2 28 65 82 70; fax: +33 3 28 65 82 44.

*E-mail address:* [Mohamad.Kassem@univ-littoral.fr](mailto:Mohamad.Kassem@univ-littoral.fr) (M. Kassem)

### **Keywords**

Sulfide glasses, XRD, DSC, SEM, Conductivity, Sensors, Ion selective measurements

### **Abstract**

Lead doped chalcogenide glass compositions, in the pseudo-ternary AgI-PbS-As<sub>2</sub>S<sub>3</sub>, were examined as active membrane materials for the construction of Pb(II) ion-selective sensors, Pb(II)-ISE. The basic glass properties of the synthesised bulk samples such as vitreous state, macroscopic, thermal and electric properties were studied. To this end, several techniques were used, including X-ray powder diffraction, density measurements, differential scanning calorimetry, scanning electron microscopy and impedance complex spectroscopy. It is found that the density increases with increased AgI and PbS contents. The glass transition temperatures for the studied compositions were also reported. The electrical measurement show the conductivity increases with increasing AgI content. Meanwhile, for the glasses with same AgI content and increasing

PbS content, the conductivity decreases. For the fabricated sensors, several key analytical parameters were investigated to evaluate the different glass compositions as active membranes in Pb(II)-ISE, including detection limit, sensitivity, linearity, ionic selectivity (in the presence of  $K^+$ ,  $Na^+$ ,  $Ni^{2+}$ ,  $Ca^{2+}$ ,  $Cd^{2+}$ ,  $Cu^{2+}$  and  $Hg^{2+}$  interfering cations), reproducibility and optimal pH-range.

## 1. Introduction

Industrial activities, transport and the extensive exploitation of natural resources represent a considerable source of pollution. Also, the continuous and inevitable development of these activities makes it essential to control the quality of water, soil and air. In fact, in a modern society, environmental monitoring usually forms the first pillar of environmental management policies for both chronic and accidental risks to the environment. In the field of environmental monitoring, the control of industrial heavy metal pollutants is very important because there is a direct impact on public health.

Among the heavy metals, lead (in all its form) is classified among the most toxic and as such presents long term effects on human health [1]. Lead exposure leads to neurodevelopmental effects in children, cardiovascular and renal diseases as well as haematological and reproductive effects. It impairs both the respiratory and digestive systems and inorganic lead compounds are probably carcinogenic to humans [1–6]. Consequently, the monitoring of lead ions in environment is essential, and a reliable and inexpensive mean of achieving this goal is potentiometric lead ion-selective electrodes, Pb(II)-ISE.

Many sensing agents have been reported as selective components for lead ions, e.g., ionophore doped PVC, chelates of naphthalene-1-dithiocarboxylate, Calixarenes, Crown ethers, etc. [7–15]. Potentiometric chemical sensors using metal-doped chalcogenide glasses as sensitive active membrane are also promising. Their enhanced chemical durability and stability in aggressive media [16] makes them good candidates for heavy metal detection including lead [17–23]. Accordingly, in this paper, we report the synthesis and the properties of new glasses in the pseudo-ternary AgI-PbS-As<sub>2</sub>S<sub>3</sub> system, bearing in mind their possible use as sensitive membranes of lead chemical sensors. In this regards, four bulk different glass compositions were synthesized and their

macroscopic, thermal and electric properties were characterized for the first time. The new AgI-PbS-As<sub>2</sub>S<sub>3</sub> chalcogenide glass compositions were then used for the fabrication and analytical characterization of new lead sensors, Pb(II)-ISE. In addition, the obtained analytical parameters are compared with those reported for lead sensors using different glass chemical compositions.

To resume, the objective of the present work is to characterise the newly synthesised multicomponent chalcogenide glasses and to study the analytical properties of the fabricated electrodes using the obtained glassy compositions.

## **2. Methods**

### *2.1 Glass synthesis*

Four glass compositions are obtained, in the (AgI)<sub>x</sub>(PbS)<sub>y</sub>(As<sub>2</sub>S<sub>3</sub>)<sub>z</sub> chalcogenide system ( $x + y + z = 100$  mol.%), via the classical melt-quenching technique and the compositions of the obtained glasses are shown in Table 1. To this end, lead sulfide PbS powder (99.9% pure, Sigma-Aldrich), silver iodide AgI powder along the arsenic sulfide As<sub>2</sub>S<sub>3</sub> precursors were introduced into cleaned silica tubes (10 mm ID and 1 mm wall thickness) in appropriate proportions before being sealed under vacuum ( $10^{-6}$  mbar). The AgI and As<sub>2</sub>S<sub>3</sub> components, used in the glass synthesis, were not commercially purchased and were obtained following the synthesis procedures described elsewhere [24–28]. The evacuated silica ampoules, containing the three components, were heated slowly in a rocking furnace to 850 °C at a rate of 1°C/minute and homogenized at this temperature for 48h. The furnace temperature was then decreased to 750 °C at a rate of 1°C/minute and the melt was quenched in icy salt water. The total mass of the sample compositions was 3 g.

### *2.2 Glass characterization*

The Bruker D8 advance XRD diffractometer was used to identify the amorphous nature of materials at room temperature. This latter was equipped with a copper anticathode emitting  $K\alpha$  radiation ( $\lambda = 1.5406 \text{ \AA}$ ), a LinxEye detector, a goniometer  $\theta/\theta$  and a rotating sample holder. The scattering intensities were measured over the angular range of  $10^\circ \leq 2\theta \leq 80^\circ$  with a step-size of  $0.02^\circ$  and a count time of 2 s per step. The density,  $d$ , measurements were conducted with the use of Sartorius YDK 01-0D density kit. The employed hydrostatic method used toluene as an immersion fluid and a germanium standard (Germanium density  $d_{Ge} = 5.323 \text{ g cm}^{-3}$ ).

The glass transition temperature values,  $T_g$ , of the samples were obtained using the DSC instrument, TA Q200 differential scanning calorimeter. The samples (mass of 10–15 mg) were hermetically encapsulated in a standard aluminium pan and an empty aluminium pan was served as a reference. The samples are then heated in the temperature range 25–450 °C under nitrogen flow and the heating rate employed was  $10 \text{ K min}^{-1}$ .

A JEOL JSM-7100F thermal field emission scanning electron microscope equipped with three EDX Bruker QUANTAX 800 spectrometers ( $3 \times 30 \text{ mm}^2$ ) was used to check the sample uniformity. The sample was fixed using a metallic tape before being sputter coated with gold to avoid charging under electron beam and introduced into the instrument chamber.

The total electrical conductivity values,  $\sigma$ , of the samples was measured using a Hewlett Packard 4194A impedance meter in the frequency range 100 Hz to 15 MHz and the temperature range was 25 – 130 °C. The rectangular glassy samples were polished using SiC powder ( $9.3 \mu$  grain size) and graphite was deposited on two parallel sides of the sample to form blocking electrodes for conductivity experiment. Further details concerning the measurements are presented elsewhere [24–28].

### *2.3 Electrode assembly*

The four chalcogenide glass compositions were used as active membrane materials in the fabrication of the Pb(II)-ISEs sensors. The designated electrode code along with the glass composition and the physicochemical properties of the glass active membrane materials, i.e., density and glass transition temperatures are given in Table 1 and in Figure S1. We note that the sensors Pb-ISE30 (40 mol.% AgI), Pb-ISE25(50 mol.% AgI) and Pb-ISE20 (60 mol.% AgI), belong to the same line on the diagram (wine coloured line), Figure S1. The Pb-ISE30 and Pb-ISE10 have the same silver iodide content (40 mol.% AgI). The back sides of the as-prepared glasses were polished with SiC powder (9.3  $\mu$  grain size). The ball-shaped membranes were then glued into PVC tubes using an electrical isolator epoxy resin and left to dry for few days under an infrared lamp. After this step, 2 ml of the liquid mixture Pb(NO<sub>3</sub>)<sub>2</sub>/AgNO<sub>3</sub> (0.1 M) was added inside the PVC tube; this electrolyte ensures the electrical contact between the glass membrane and the AgCl coated silver wire serving as inner reference electrode. For each composition, four electrodes were prepared. Thus, the total number of electrodes tested during this study amounts to 16. Figures S2 and S3 show an illustration of the fabricated chemical sensor with liquid contact and photos of the actual sensors obtained by the end of fabrication process, respectively.

**Table 1.** Pb(II)-ISEs : composition of the active membrane chalcogenide materials, the arsenic atomic percentage within the composition (As at.%), the designated names of the fabricated sensors, the density,  $d$ , and glass transition temperatures of the glass membranes,  $T_g$ .

<i>Composition</i> (mol.%)				<i>ISE code</i>	<i>d</i> (g.cm <sup>-1</sup> )	<i>T<sub>g1</sub></i> (°C) (± 5)	<i>T<sub>g2</sub></i> (°C) (± 5)
				(AgI) <sub>x</sub> (PbS) <sub>y</sub> (As <sub>2</sub> S <sub>3</sub> ) <sub>z</sub>			
<i>x</i>	<i>y</i>	<i>z</i>	As (at.%)				
40	10	50	28	<b>Pb-ISE10</b>	4.13(1)	106	179
60	20	20	15	<b>Pb-ISE20</b>	5.44(2)	103	–
50	25	25	18	<b>Pb-ISE25</b>	5.31(1)	119	–
40	30	30	20	<b>Pb-ISE30</b>	5.13(2)	133	–

*Uncertainties in the last digit(s) of the parameter are given in parentheses.*

## 2.4 Potentiometric measurements

Two electrodes were used in the electrochemical cell presented in Figure 1, i.e., the reference (Ag,AgCl | KCl<sub>(saturated)</sub>) electrode and the working Pb(II)-ISE electrode.

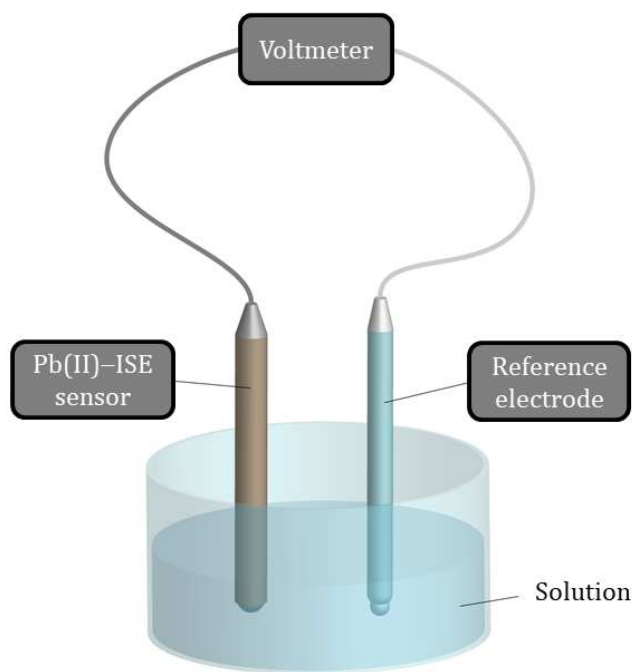


**Figure 1.** Schema of the simplified electrochemical cell used for Potentiometric measurements.

The KNO<sub>3</sub> (0.1 M) was used as a salt bridge. The potentiometric measurements were conducted in magnetically stirred solutions at 20 °C. Standard solutions of lead were prepared from 1 M Pb(NO<sub>3</sub>)<sub>2</sub> by consecutive dilution with ultrapure water and the ISEs calibrations were performed in the concentration range from 10<sup>-8</sup> – 10<sup>-3</sup> mol.L<sup>-1</sup> Pb<sup>2+</sup>-ions.



The pH effect on the electrode performance was examined in solutions with constant concentration of the potential-determining ions; HCl or NaOH were added to alter the hydrogen ions concentration. Selectivity coefficients were determined using the two

versions of the mixed solutions method under (i) a constant concentration of the interfering ions (in case of  $K^+$ ,  $Na^+$ ,  $Ni^{2+}$  and  $Ca^{2+}$  ions) and a variable concentration of the  $Pb^{2+}$ -ions or (ii) a variable concentration of the interfering ions (in case of  $Cu^{2+}$ ,  $Cd^{2+}$  and  $Hg^{2+}$ ) and a constant concentration of the  $Pb^{2+}$ -ions.

### 3. Results and discussion

#### 3.1. Physicochemical properties of the active membrane chalcogenide glasses

XRD diffraction patterns of the four active membrane compositions, synthesized in the  $(AgI)_x(PbS)_y(As_2S_3)_z$  chalcogenide system, are presented in Figure 2. The absence of Bragg peaks and the presence of the broad diffraction features confirm the amorphous nature of the obtained compositions. The properties of the membranes are therefore intrinsic glass properties not related to a possible presence of crystalline phases.

The measured density values of the investigated glasses in the  $(AgI)_x(PbS)_y(As_2S_3)_z$  system are in the range 4.13(1) – 5.44(2)  $g\ cm^{-3}$ , Table 1. The increase of AgI or PbS content in the membrane compositions leads to increased density values. This is not surprising considering that the densities of the two crystalline forms of silver iodide ( $d_{\alpha-AgI} = 6.12\ g\ cm^{-3}$  and  $d_{\beta-AgI} = 5.68\ g.cm^{-3}$  [29]) and of crystalline lead sulfide ( $d_{PbS} = 7.6\ g\ cm^{-3}$  [29]) are higher than those of the  $As_2S_3$  host glass ( $d_{g-As_2S_3} = 3.18\ g\ cm^{-3}$ ) or crystalline orpiment  $As_2S_3$  ( $d_{c-As_2S_3} = 3.46\ g\ cm^{-3}$  [30]). The glass membranes with the equivalent PbS/ $As_2S_3$  ratio, i.e. Pb-ISE20 (60 mol.% AgI), Pb-ISE25 (50 mol.% AgI) and Pb-ISE30 (40 mol.% AgI), show that the density increases from 5.13(2) to 5.44(2)  $g\ cm^{-3}$  with increasing AgI content. Comparing the two membranes with same AgI content, i.e. Pb-ISE10 and Pb-ISE30, the former with lower PbS content presents a lower density value (4.13(1)  $g\ cm^{-3}$ ).

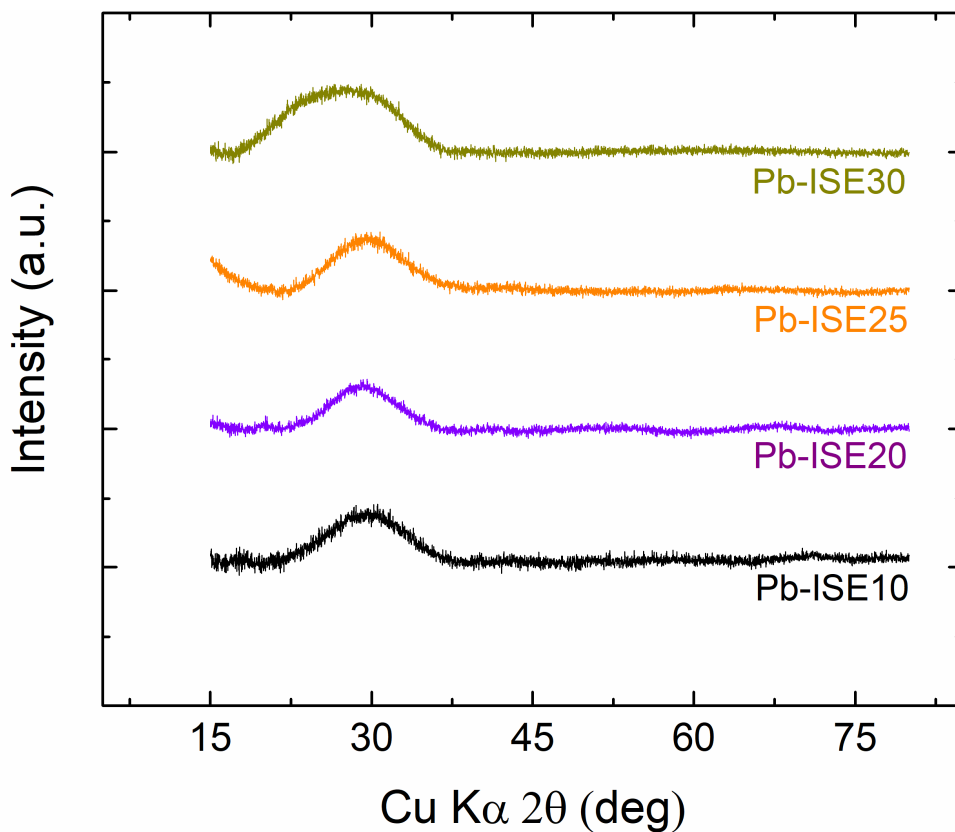


**Figure 2.** Diffraction XRD patterns of the four different compositions used as active membranes in the lead chemical sensors.

In relation to DSC measurements, a single  $T_g$  was observed for the glass membranes used in sensors Pb-ISE20, Pb-ISE25 and Pb-ISE30. The results are reported in Figure 3 and Table 1. This indicates a homogenous glass nature, on macroscopic and mesoscopic scale, for these three compositions. Meanwhile, the two glass transition temperatures ( $T_{g1}$  and  $T_{g2}$ ), recorded for the glass membrane of the sensor Pb-ISE10, is an indication of a non-homogenous nature, Figure 3. The two glass transition values are  $106^\circ\text{C}$  and  $179^\circ\text{C}$  and are plotted in the inset of Figure 3 in green. The SEM studies, conducted on the Pb-ISE10 and Pb-ISE20 glass samples, confirm the DSC results (Figure S4). The Pb-ISE10 glass was phase separated; it contained dark spherical particles that are rich in arsenic as indicated from the EDX. Meanwhile, Pb-ISE20 glass was rather smooth and homogeneous.

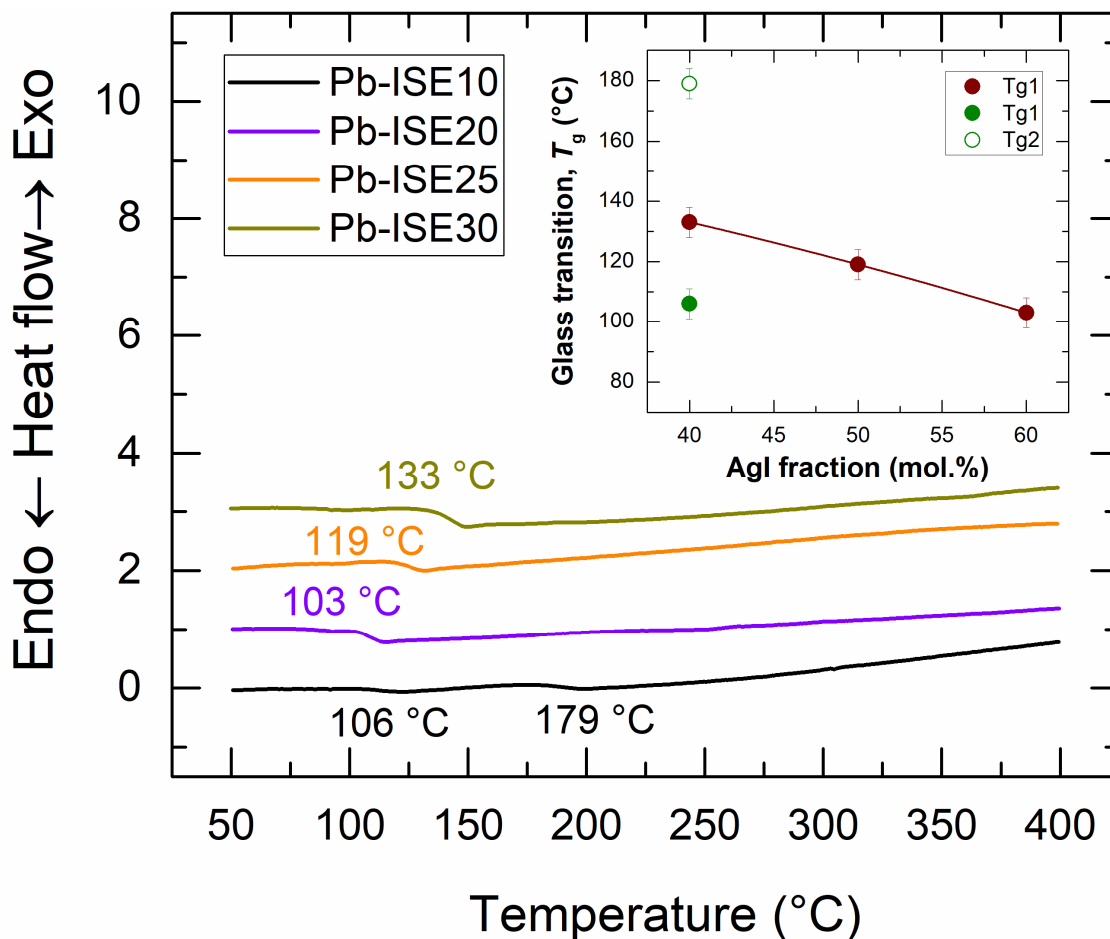


**Figure 3.** DSC traces of the four glass compositions, obtained by melt quenching, used as active membranes in the lead chemical sensors. The inset shows the evolution of the glass transition temperature as a function of silver iodide molar fraction. The line in the inset is drawn as guide to the eyes.

$T_g$  values vary with the glass composition. The glass membranes with the equivalent PbS/As<sub>2</sub>S<sub>3</sub> ratio, i.e., Pb-ISE20 (60 mol.% AgI), Pb-ISE25 (50 mol.% AgI) and Pb-ISE30 (40 mol.% AgI), show that glass transition decreases with increasing AgI content from 133 °C to 103 °C (inset of figure 3). The  $T_g$  decrease can be explained by fragmentation of the glass network with reduced arsenic atomic fraction. Short oligomeric sulphur chains diminish the network connectivity [27,31] while replacing the bridging sulphur in corner-sharing CS-AsS<sub>3/2</sub> pyramids. On the contrary, the addition of PbS leads to an increase of  $T_g$  values; the two membranes with same silver iodide content (Pb-ISE10 and

Pb-ISE30) show that the glass transition  $T_{g1}$  goes up from 106 °C to 133 °C. This can be explained by increased crosslinking degree of the glass network upon PbS addition (fourfold Pb vs. threefold As). Similar behaviour was previously reported in the pseudo-binary  $(\text{PbS})_x(\text{As}_2\text{S}_3)_{1-x}$  glass system ( $T_g$  presented a slight increase with increasing PbS content) [32,33].

### 3.2. Electrical properties

The room temperature electrical conductivity  $\sigma_{298}$  and the activation energy  $E_\sigma$  of the 4 membranes are displayed in Figure 4. The electrical conductivity  $\sigma_{298}$  increases by 2.5 orders of magnitude with increasing AgI content for the membranes with the equivalent PbS/As<sub>2</sub>S<sub>3</sub> ratio, i.e.,  $\sigma_{298}$  (Pb-ISE20) >  $\sigma_{298}$  (Pb-ISE25) >  $\sigma_{298}$  (Pb-ISE30), Figure 4(a). This is accompanied by a decrease in the activation energy from 0.449(3) eV to 0.312(5) eV, Figure 4(b). In regards to these three compositions, the conductivity values are comparable to the glass compositions  $x = 0.4, 0.5$  and  $0.6$  in the  $(\text{AgI})_x(\text{HgS})_{0.5-x/2}(\text{As}_2\text{S}_3)_{0.5-x/2}$  system, respectively [34]. The values are typical of the modifier-controlled domain where the transport parameters depend essentially on the modifier content and are related to the nature of mobile cations ( $\text{Ag}^+$ ,  $\text{Cu}^+$ , etc.) and its chemical form [35, 36]. In this domain, the previously silver-related isolated percolation clusters become predominant, cover the whole volume of the glass and form preferential conduction pathways responsible for high conductivity [37]. As previously [34], we suggest that the high  $\text{Ag}^+$  ionic mobility of the lead doped system in the modifier controlled domain is probably the results of the interconnected tetrahedral  $(\text{AgI}_{2/2}\text{S}_{2/2})_n$  chains or  $\text{AgI}_{3/3}\text{S}_{1/2}$  mixed tetrahedral present in the glass network. Further studies using high-energy X-ray or neutron scattering are necessary to verify this hypothesis.

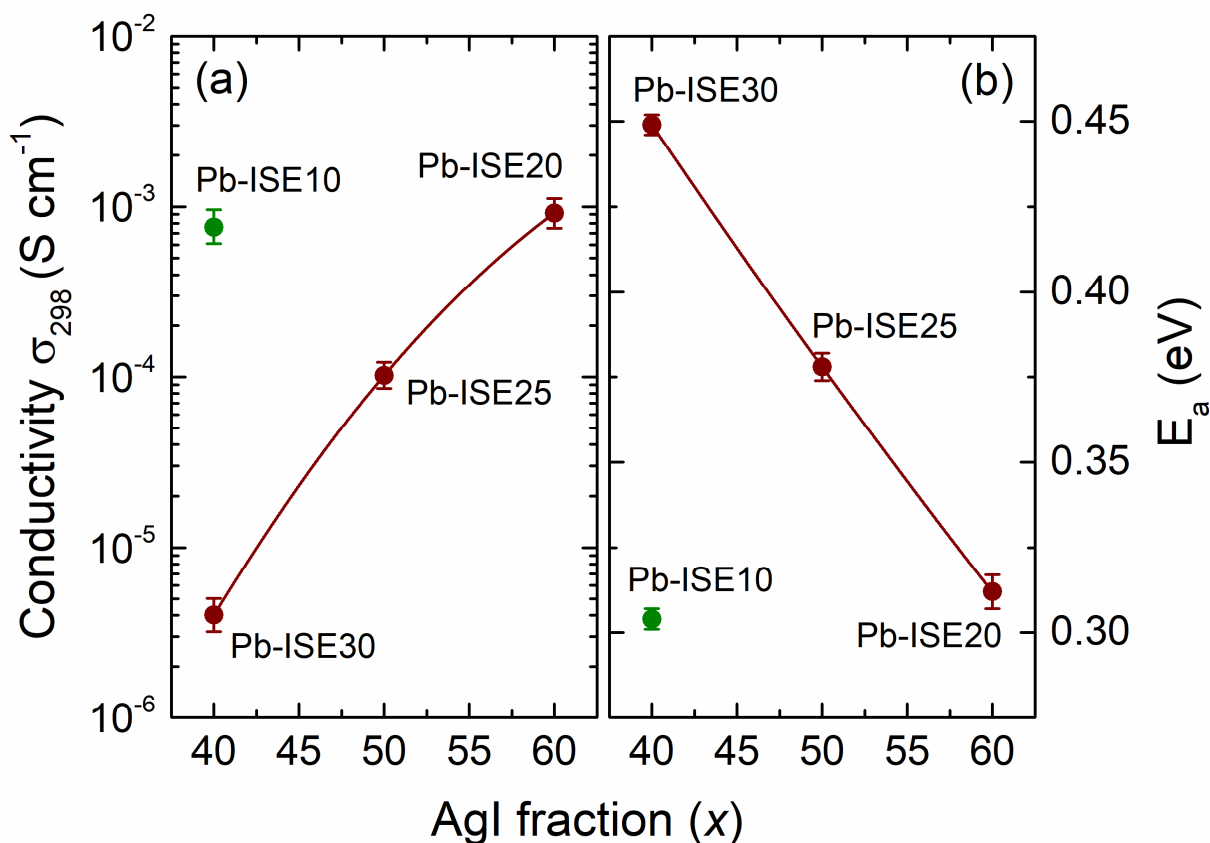


**Figure 4.** (a) The room temperature conductivity and (b) activation energy of the four compositions used as active membranes in the lead chemical sensors. The wine coloured points represent the electrodes that belong to the same line on the diagram (Fig. S1). The lines are drawn as guides to the eyes.

The results also show that the conductivity is not only related to silver concentration. For example, the membranes Pb-ISE10 (~15.4 at.% Ag) and Pb-ISE20 (~23.07 at.% Ag) present a comparable conductivity value despite a difference of ~8 at.% in silver content. Meanwhile, the membranes Pb-ISE10 (~15.4 at.% Ag) and Pb-ISE30 (~13.8 at.% Ag) show a difference in conductivity exceeding two orders of magnitude in favour of the first membrane despite the low difference in at.% Ag (~1.6 at.%). This suggests that the PbS content is playing a role with regards to the conductivity values and that lead content in the membranes affects the Ag<sup>+</sup> ion mobility responsible for ionic transport in glasses. Previously, it was reported that the presence of immobile or slow ions restricts the number of silver accessible empty sites and thus affects the Ag<sup>+</sup> ion dynamics and

reduces the ionic conductivity [24]. Comparing the membranes Pb-ISE30 (10.3 at.% Pb), Pb-ISE20 (~7.7 at.% Pb) and Pb-ISE10 (~3.8 at.% Pb), one can easily conclude that the ionic conductivity is reduced with increasing lead content.

### 3.3. Characterization of the lead sensor

The assembled lead sensors were diagnosed for a number of parameters related to the calibration functions: detection limit, slope, linear response range, selectivity coefficient in presence of interfering ions ( $K_{Pb^{2+},M^{Y+}}$ ), reproducibility and optimal pH-range.

#### 3.3.1. Slope, linearity and detection limit

The potential response of the sensors as a function of the  $Pb^{2+}$  ions was investigated in the concentration range  $10^{-8} - 10^{-3}$  M, Figure 5. Table 2 summarizes the obtained data of the slope, the linear response range as well as the detection limit for all assembled sensors.

**Table 2.** Electrochemical parameters of different Pb(II)-ISEs

	<b>Pb-ISE10</b>	<b>Pb-ISE20</b>	<b>Pb-ISE25</b>	<b>Pb-ISE30</b>
<b>Slope (mV.dec<sup>-1</sup>)</b>	12.9(2)	22.5(4)	21.3(7)	18.3(9)
<b>Linear range (mol.L<sup>-1</sup>)</b>	$2 \times 10^{-4} - 10^{-3}$	$2 \times 10^{-5} - 10^{-3}$	$2 \times 10^{-5} - 10^{-3}$	$10^{-4} - 10^{-3}$
<b>Detection limit (mol.L<sup>-1</sup>)</b>	$3.9(2) \times 10^{-5}$	$3.3(1) - 5.7(1) \times 10^{-6}$	$6.1(3) \times 10^{-6}$	$1.8(2) \times 10^{-5}$

The membranes Pb-ISE10 and Pb-ISE30 exhibit detection limits in the micromolar concentration range,  $3.9(2) \times 10^{-5}$  and  $1.8(2) \times 10^{-5}$ , limited linear responses in the range  $\sim 10^{-4} - 10^{-3}$  M as well as low slopes of  $\sim 12.9$  and  $\sim 18.3$  mV.decade<sup>-1</sup>, respectively. The calibration parameters improve for the Pb-ISE20 and Pb-ISE25 membranes. The detection limits are in the concentration range around  $\sim 10^{-6}$  M and the lowest value recorded was  $3.3 \times 10^{-6}$  M for the Pb-ISE20 sensor. The detection limit values are better than those reported previously [22], i.e.,  $1 \times 10^{-4}$  or  $1 \times 10^{-5}$  depending on composition,

and comparable to those of reference [38] ( $3.5\text{--}7.9\times 10^{-6}$ ) and lower ( $1\text{--}3\times 10^{-7}$ ,  $1\times 10^{-7}$  and  $5\text{--}6\times 10^{-7}$ ) than those reported in references [21, 23, 19], respectively. The linear range is extended over 1-2 order of magnitude and the calculated slopes are 22.5 and 21.3 mV/decade, respectively. All the sensors present slopes different from the theoretical value ( $\approx 29.6$  mV/ decade). It is clear that the sensors Pb-ISE20 present the best results in terms of sensitivity (the highest slope) and detection limit (the lowest). As such, these Pb-ISE20 membranes will be used for further potentiometric characterizations.

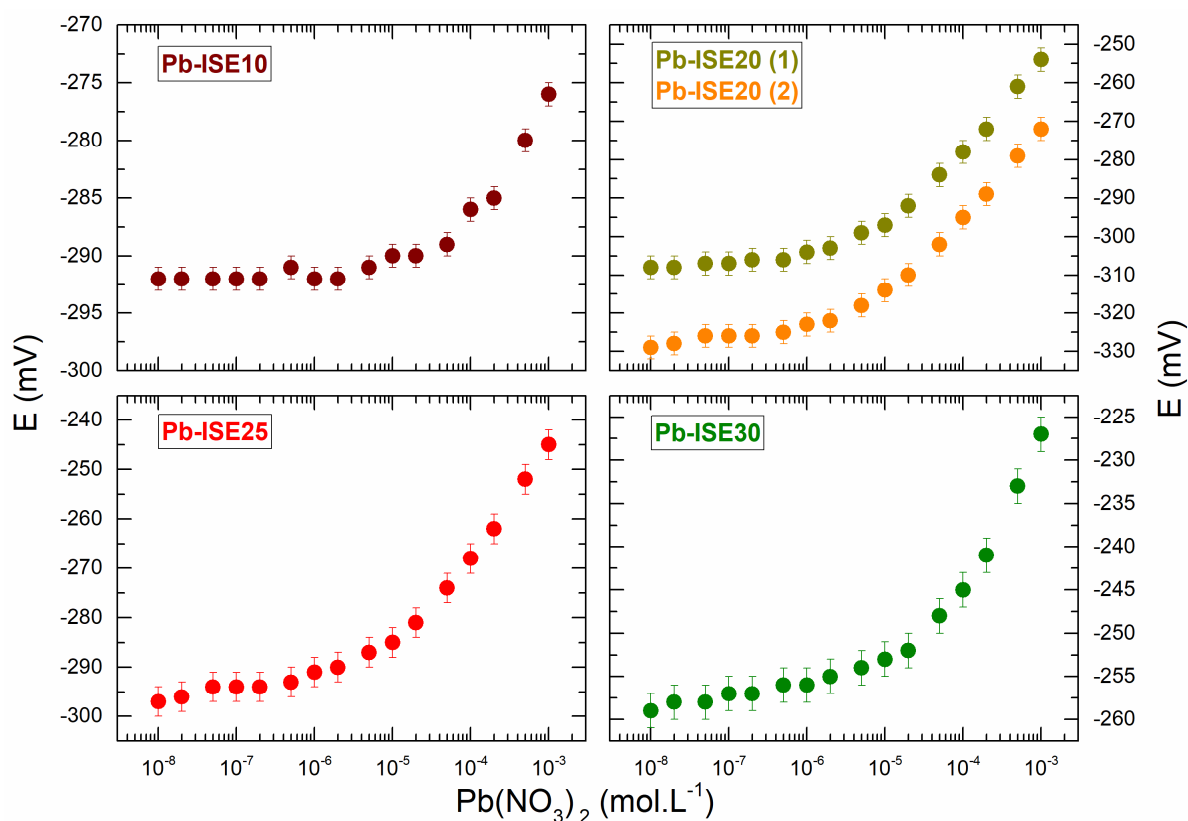


**Figure 5:** Selected calibration curves for the fabricated  $\text{Pb}^{2+}$  sensors. In case of the sensor labeled Pb-ISE20, the curves belong to two different sensors.

The mechanism of ionic sensitivity is based on direct exchange of  $\text{Pb}^{2+}$  ions between the analyzed solution and the modified surface layer of a chalcogenide glass membrane shown earlier by X-ray photoelectron spectroscopy and tracer exchange experiments

[39-41]. Basically, it is similar to the pH or alkali ion response of an oxide glass electrode in aqueous solution [42]. However, the question arises about the origin of the difference in performance for different sensors. We note that the optimal sensor performance is a complex function of several parameters. Insufficient ionic sensitivity of the Pb-ISE10 sample is related to low lead sulfide content (10 mol.%) and inhomogeneous glass nature reflected by two glass transition temperatures and SEM studies. The Pb-ISE30 sample has the highest PbS content (30 mol.%) but simultaneously the lowest ionic conductivity ( $4 \times 10^{-6} \text{ S cm}^{-1}$ ). Consequently, the ion-exchange current density at the glass/solution interface is lower than for both Pb-ISE25 and Pb-ISE20 membranes and, as a result, the sensor performance is also insufficient. The last two membranes (Pb-ISE25 and Pb-ISE20) are rather close to each other and are characterized by two contrasting trends (an increase in the PbS content is accompanied by a decrease in the ionic conductivity). Glasses with higher silver iodide content are also more chemically stable; a better performance of Pb-ISE20 seems to be related to higher AgI fraction (60 mol.%).

### *3.3.2. Selectivity coefficient $K_{\text{Pb}^{2+}, \text{M}^{y+}}$ in standard solutions*

The selective response of a sensor for the  $\text{Pb}^{2+}$  primary ion, in the presence of interfering ions, is an essential parameter which attests to the utility of that sensor to be used in real sample measurements. The selectivity coefficients of Pb-ISE20 sensor were determined in the presence of alkali ( $\text{K}^+$ ,  $\text{Na}^+$ ) and alkali-earth or heavy-metal ions ( $\text{Ni}^{2+}$ ,  $\text{Ca}^{2+}$ ,  $\text{Cu}^{2+}$ ,  $\text{Cd}^{2+}$ ,  $\text{Hg}^{2+}$ ). The selectivity coefficients  $K_{\text{Pb}^{2+}, \text{M}^{y+}}$  for the cations  $\text{K}^+$ ,  $\text{Na}^+$ ,  $\text{Ni}^{2+}$  and  $\text{Ca}^{2+}$  were determined via a mixed solution method using a constant concentration of the interfering ions and a variable concentration of the  $\text{Pb}^{2+}$  ion. In case of the strongly interfering ions  $\text{Cu}^{2+}$ ,  $\text{Cd}^{2+}$  and  $\text{Hg}^{2+}$ , the mixed solution method employed with a fixed

concentration of primary  $\text{Pb}^{2+}$  ion and a varying concentration of interfering ion. The potentiometric selectivity coefficients ( $K_{\text{Pb}^{2+}, \text{M}^{y+}}$ ) of various ions, presented in Table 3 and Table 4, were calculated via the Nikolsky–Eisenman equation [43] :

$$E = E^0 + \frac{RT}{2F} \ln (a_{\text{Pb}^{2+}} + K_{\text{Pb}^{2+}, \text{M}^{y+}} \times a_{\text{M}^{y+}}) \quad (1)$$

where R is the gas constant, T is the temperature in Kelvin, F is the Faraday constant ,  $a_{\text{Pb}^{2+}}$  is the activity of primary ion,  $a_{\text{M}^{y+}}$  is the activity of interfering  $\text{M}^{y+}$  ions and  $y^+$  are charge numbers of various interfering ions.

**Table 3.** Selectivity coefficients of Pb-ISE20 with respect to the interfering ions  $\text{K}^+$ ,  $\text{Na}^+$ ,  $\text{Ni}^{2+}$  and  $\text{Ca}^{2+}$ . The measurements were conducted using a constant concentration of interfering ions.

Interfering ion	Interfering ion concentration	Selectivity coefficient $K_{\text{Pb}^{2+}, \text{M}^{y+}}$
<b>Potassium ion <math>\text{K}^+</math></b>	$10^{-1}$ M	$3.5(2) \times 10^{-5}$ M
	$10^{-2}$ M	$8(2) \times 10^{-4}$ M
	$10^{-3}$ M	$3.9(1) \times 10^{-3}$ M
<b>Sodium ion <math>\text{Na}^+</math></b>	1 M	$2(1) \times 10^{-5}$ M
	$10^{-1}$ M	$6(2) \times 10^{-5}$ M
<b>Nickel ion <math>\text{Ni}^{2+}</math></b>	$10^{-1}$ M	$4.0(1) \times 10^{-5}$ M
<b>Calcium ion <math>\text{Ca}^{2+}</math></b>	$10^{-1}$ M	$2.5(2) \times 10^{-4}$ M

The selectivity coefficients indicate that the sensor is selective for  $\text{Pb}^{2+}$  ion in the presence of  $\text{K}^+$ ,  $\text{Na}^+$ ,  $\text{Ni}^{2+}$ ,  $\text{Ca}^{2+}$  and  $\text{Cd}^{2+}$  interfering ions. Meanwhile, the interfering ions  $\text{Cu}^{2+}$  and  $\text{Hg}^{2+}$  display strong interfering effect. Selectivity coefficient data were reported in references [21], [23] and [38]. Similarly to our results, the sensors in references [21] and [23] were not selective for the  $\text{Cu}^{2+}$  and  $\text{Hg}^{2+}$  interfering ions. In Ref. [38], the sensor was not tested for  $\text{Hg}^{2+}$  ions but it was selective for  $\text{Cu}^{2+}$  ions.

**Table 4.** Selectivity coefficients of Pb-ISE20 with respect to the interfering ions Cu<sup>2+</sup>, Cd<sup>2+</sup> and Hg<sup>2+</sup>. The measurements obtained using a constant concentration of Pb<sup>2+</sup> ions.

Interfering ion	Pb <sup>2+</sup> primary ion concentration	Selectivity coefficient $K_{Pb^{2+}, M^{y+}}$
<b>Copper ion Cu<sup>2+</sup></b>	10 <sup>-1</sup> M	3(2) × 10 <sup>3</sup> M
	10 <sup>-2</sup> M	1.3(3) × 10 <sup>3</sup> M
	10 <sup>-3</sup> M	5(1) × 10 <sup>2</sup> M
	10 <sup>-4</sup> M	1.3(3) × 10 <sup>2</sup> M
<b>Cadmium ion Cd<sup>2+</sup></b>	10 <sup>-2</sup> M	< 10 <sup>-8</sup> M
	10 <sup>-4</sup> M	< 10 <sup>-8</sup> M
	10 <sup>-6</sup> M	1.1(2) × 10 <sup>-2</sup> M
	10 <sup>-8</sup> M	4(1) × 10 <sup>-4</sup> M
<b>Mercury ion Hg<sup>2+</sup></b>	10 <sup>-1</sup> M	8.9(1) × 10 <sup>4</sup> M
	10 <sup>-3</sup> M	1.9(1) × 10 <sup>3</sup> M
	10 <sup>-5</sup> M	2.8(2) × 10 <sup>1</sup> M
	10 <sup>-7</sup> M	3.9(1) × 10 <sup>-1</sup> M

### 3.3.3. pH influence

Determining the optimal pH working range (i.e., the range where the potential of the sensor is invariant for a given concentration of Pb<sup>2+</sup>), is an essential potentiometric measurement. Figure 6 illustrates the influence of pH on the Pb-ISE20 sensor. The measurements were performed, in the pH range 1 to 8, using constant Pb<sup>2+</sup> primary cation concentrations and two different concentrations were employed, i.e., 1 × 10<sup>-2</sup> M and 1 × 10<sup>-5</sup> M Pb(NO<sub>3</sub>)<sub>2</sub>. One clearly observes that the potential is constant in the pH range 2.5–4.8 for the diluted lead concentration (1 × 10<sup>-5</sup> M Pb(NO<sub>3</sub>)<sub>2</sub>). The working pH ranges improves as the concentration of the Pb(NO<sub>3</sub>)<sub>2</sub> solution is increased (1 × 10<sup>-2</sup> M) and the recorded pH range is 1.9 ≤ pH ≤ 5.0. The decrease in the sensor potential values at pH > 5 and pH < 2 is mostly due to the hydrolysis of Pb<sup>2+</sup> ions in solution and to changes in the liquid junction potential, respectively. The sensor presents a wider working pH range in comparison to that reported in ref. [38], i.e., 1.5–2.5. The references [21] and [23] reported pH ranges of 2–5.5 and 2–6, respectively.

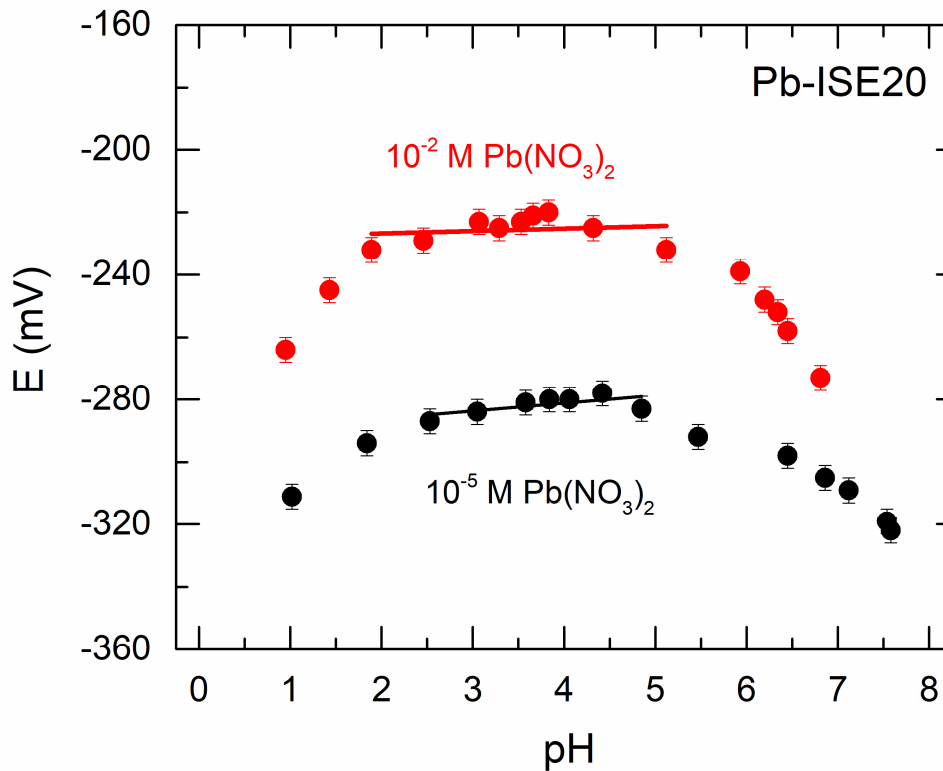


**Figure 6.** pH values of the sensor Pb-ISE20 traced as a function of potential of  $\text{Pb}(\text{NO}_3)_2$  solution and for two different concentrations of  $10^{-2}$  M and  $10^{-5}$  M. The lines are drawn as guides to the eyes.

### 3.3.4. Reproducibility of the electrode potential

Figure 7 shows the reproducibility of the Pb-ISE20 sensor for six different concentrations of the  $\text{Pb}(\text{NO}_3)_2$  solution, i.e., the concentration domain  $10^{-8}$  –  $10^{-3}$  M. The reproducibility parameter, primordial for continuous in situ measurements, was investigated using a series of consecutive measurements in standard solutions [44,45]. The sensor measures the potential of the solution of a given concentration for a period 2 minutes and is then placed in the open air for another 2 minutes. This procedure is repeated several times for about one hour in order to study the reproducibility of the potential as a function of time. The mean value of the potential and especially the mean square deviation of this value give us a good estimate of the stability and reproducibility of the response of the sensor. Figure 7 shows that the change in potential, during

consecutive measurements, is  $\pm 2-3$  mV and that the reproducibility does not depend on the concentration of the primary  $\text{Pb}^{2+}$  ions.

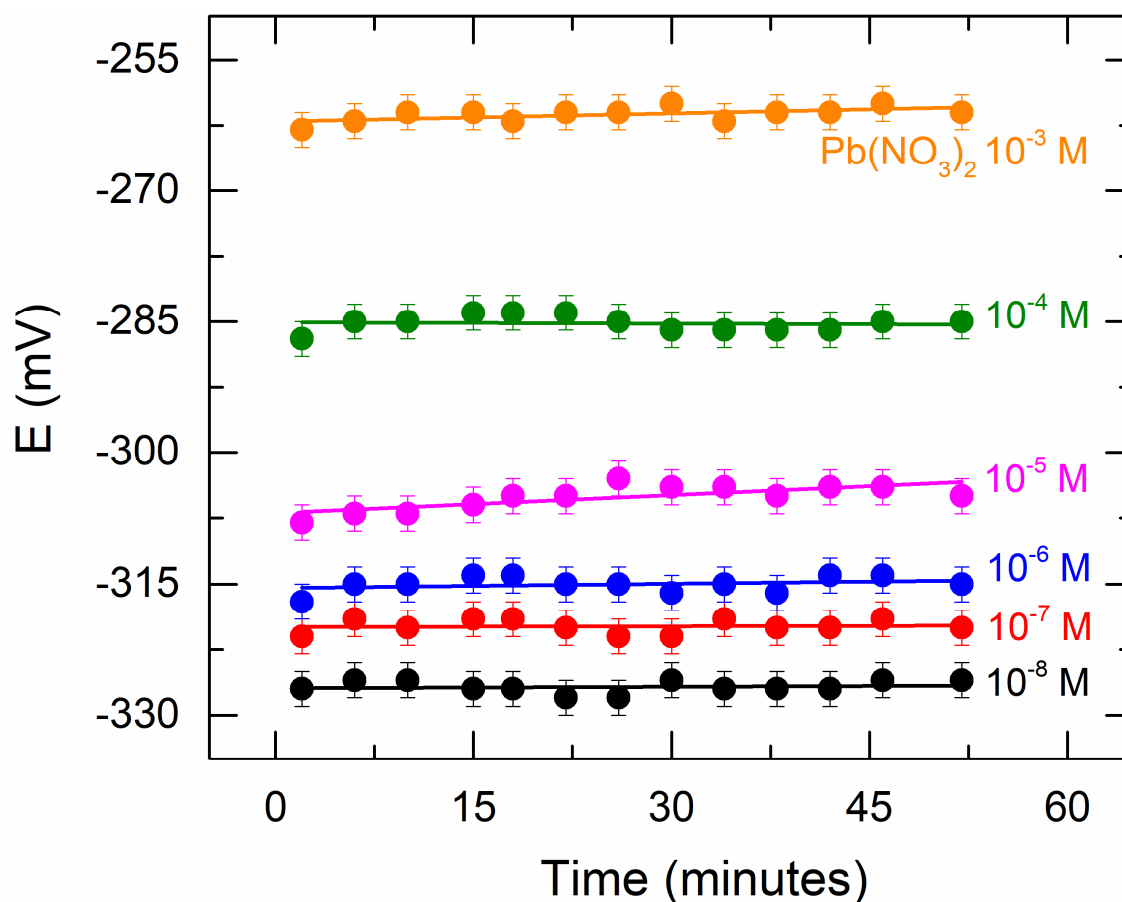


**Figure 7.** The reproducibility of the sensor Pb-ISE20 in different concentrations of the standard lead nitrate  $\text{Pb}(\text{NO}_3)_2$  solution. The lines are drawn as guides to the eyes.

#### 4. Conclusion

Four different glass compositions were synthesised and characterised in the pseudo-ternary  $(\text{AgI})_x(\text{PbS})_y(\text{As}_2\text{S}_3)_z$  system. For all compositions, the density increases with increasing AgI and PbS contents. The thermal studies show that the three glass compositions, Pb-ISE20 (60 mol.% AgI; 20 mol.% PbS), Pb-ISE25 (50 mol.% AgI; 25 mol.% PbS) and Pb-ISE30 (40 mol.% AgI; 30 mol.% PbS), are homogenous in contrary to the Pb-ISE10 one (40 mol.% AgI; 10 mol.% PbS) which presented two glass transition values. Impedance measurements show that the room temperature conductivity

increases by 2.5 orders of magnitude with increasing AgI concentration from  $4.01 \times 10^{-6}$  to  $9.17 \times 10^{-4}$  S.cm<sup>-1</sup>. This increase is accompanied by a consecutive decrease in the activation energy from 0.449 eV to 0.312 eV. The fourth Pb-ISE10 composition presents an ionic conductivity comparable to that in Pb-ISE20 despite the evident difference in silver iodide concentration. This is attributed to the fact that the latter is Pb-rich which affects the Ag<sup>+</sup> ion dynamics by restricting the number of silver accessible empty sites and thus limiting the ionic conductivity. Pb(II)-ISEs were prepared from the above mentioned compositions. Among the various sensors, Pb-ISE20 demonstrated the best results in terms of detection limits, linearity and slope. It shows an excellent reproducibility, good pH working range and good selectivity and reversibility to Pb<sup>2+</sup> ions in the presence of K<sup>+</sup>, Na<sup>+</sup>, Ni<sup>2+</sup>, Ca<sup>2+</sup> and Cd<sup>2+</sup> interfering cations. However, the Pb-ISE20 sensor was sensitive to Cu<sup>2+</sup> and Hg<sup>2+</sup> interfering ions.

#### **ORCID ID**

Mohammad Kassem <https://orcid.org/0000-0003-0512-0004>

#### **Acknowledgments**

This work was supported by the Région Hauts de France and the Ministère de l'Enseignement Supérieur et de la Recherche (CPER Climibio) as well as by the European Fund for Regional Economic Development. This work was also partly supported by Agence Nationale de la Recherche (ANR, France) under Grant No. ANR-15-ASTR-0016-01.

#### **Funding Information**

The Ph.D. work of Bouthayna Alrifai (First co-author) is co-funded by the Université du Littoral Côte d'Opale (ULCO) and the Lebanese University.

## References

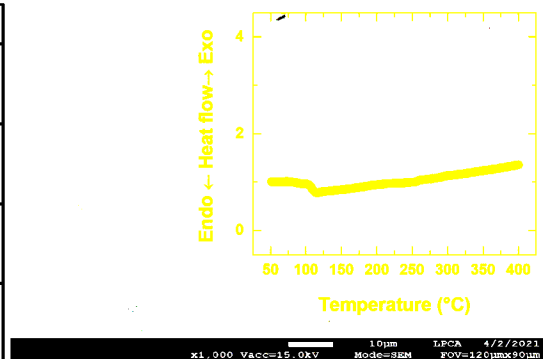
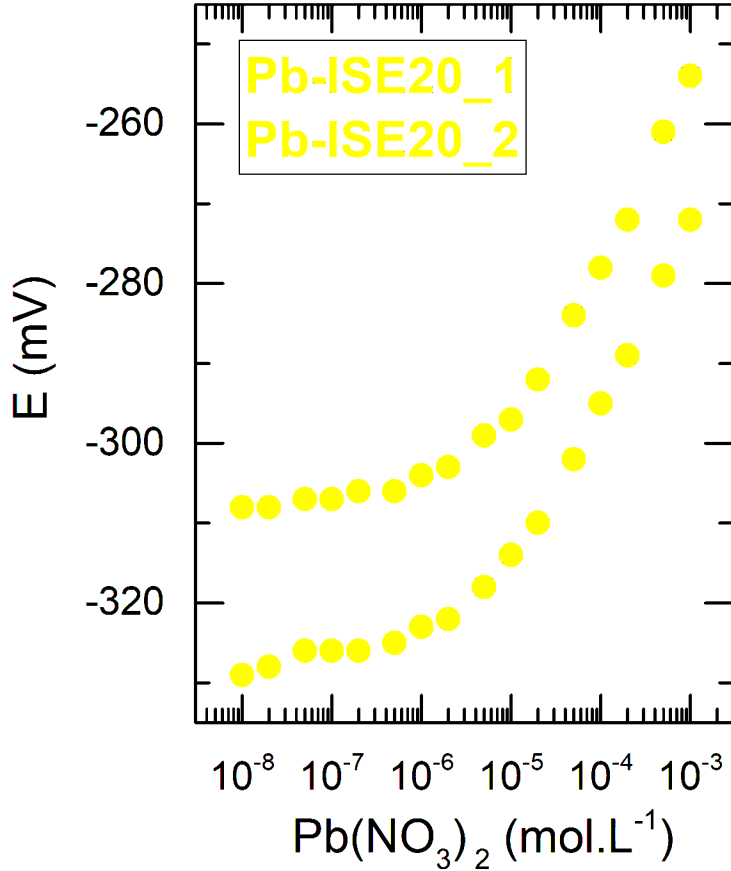
- [1] World Health Organization. Preventing disease through healthy environments: exposure to lead: a major public health concern, 2019.
- [2] World Health Organization. Recycling used lead-acid batteries: health considerations. Geneva: World Health Organization, 2017.
- [3] UNEP. Final review of scientific information on lead. Nairobi: United Nations Environment Programme, Chemicals Branch, 2010.
- [4] Inorganic and organic lead compounds. IARC Monographs for the Evaluation of Carcinogenic Risks to Humans, Vol. 87. Lyon (FR): International Agency for Research on Cancer, 2006.
- [5] H.G. Preuss, A review of persistent, low-grade lead challenge: neurological and cardiovascular consequences, *J Am Coll Nutr*, 12 (1993) 246-254.
- [6] Agency for Toxic Substances and Disease Registry (ATSDR). Toxicological profile for lead. Atlanta: US Department of Health and Human Services, Public Health Service, 2007.
- [7] S. Sadeghi, G.R. Dashti, M. Shamsipur, Lead-selective poly(vinyl chloride) membrane electrode based on piroxicam as a neutral carrier, *Sens. Actuators, B, Chem.*, 81 (2002) 223–228.
- [8] V.K. Gupta, A.K. Jain, Pankaj Kumar, PVC-based membranes of *N,N'*-dibenzyl-1,4,10,13-tetraoxa-7,16-diazacyclooctadecane as Pb(II)-selective sensor. *Sensors and Actuators B*, 120 (2006) 259-265
- [9] K. Ren, Metal chelates as membrane active components in ion selective electrodes, *Chem. Anal.*, 38 (1993) 83–93.

- [10] Vaishali S. Bhat, Vijaykumar S. Ijeri, Ashwini K. Srivastava, Coated wire lead(II) selective potentiometric sensor based on 4-*tert*-butylcalix[6]arene. *Sensors and Actuators B*, 99 (2004) 98–105.
- [11] A.K. Jain, V.K. Gupta, L.P. Singh, J.R. Raison, A comparative study of Pb<sup>2+</sup> selective sensors based on derivatized tetrapyrazole and calix[4]arene receptors. *Electrochimica Acta*, 51 (2006) 2547–2553
- [12] A.S. Attiyat, G.D. Christian, C.V. Cason, R.A. Bartsch, Benzo-18-crown-6 and its lariat ether derivatives as ionophores for potassium, strontium and lead ion-selective electrodes, *Electroanalysis*, 4 (1992) 51–56.
- [13] W. Hasse, B. Ahlers, J. Reinbold, K. Cammann, Lead hydroxide ionselective membrane electrode based on crown ethers, *Sens. Actuator B*, 19 (1994) 383–386.
- [14] E.A. Novikov, L.K. Shpigun, Y.A. Zolotov, Lead selective electrodes based on macrocyclic reagents, *Zh. Anal. Khim.*, 42 (1987) 885–890.
- [15] V. Tyagi, A.K. Jain, Use of bismuth tungstate based solid membrane as lead(II) ion-selective electrodes, *Indian J. Chem.*, 29A (1990) 608–609.
- [16] Z.U. Borisova. *Glassy Semiconductors*. New York: Plenum press, 1981, pp. 505.
- [17] A.E. Owen, Chalcogenide glasses as ion-selective materials for solid-state electrochemical sensors, *J. Non-Cryst. Solids*, 35-36 (1980) 999–1004.
- [18] C. Brohnke, J.P. Malugani, A. Saida, G. Robert, Conductivite electrique et selectivite ionique des verres AgPO<sub>3</sub>-MI<sub>2</sub> et AgAsS<sub>2</sub>-MI<sub>2</sub> avec M = Pb, Hg, *Electrochimica Acta.*, 26 (1981) 1137–1142.
- [19] Yu.G. Vlasov, E.A. Bychkov, A.V. Legin, Mechanism studies on lead ion-selective chalcogenide glass sensors, *Sensors and Actuators B*, 10 (1992) 55–60.

- [20] Yu.G. Vlasov, E.A. Bychkov, A.M. Medvedev, Copper ion-selective chalcogenide glass electrodes: Analytical characteristics and sensing mechanism, *Analytica Chimica Acta.*, 185 (1986) 137–158.
- [21] Yu.G. Vlasov, E.A. Bychkov, Ion-Selective Chalcogenide Glass Electrodes. *Ion-selective Electrode Rev.*, 9 (1987) 5–93
- [22] R. Tomova, R. Stoycheva-Topalova, A. Buroff, Ion-selective membranes based on chalcogenide glasses. *Journal of Optoelectronics and Advanced Materials*, 7(3) (2005) 1399–1406.
- [23] Yu .G. Mourzina, M.J. Schöning, J. Schubert, W. Zander, A. Legin, Yu.G. Vlasov, P. Kordos, H. Lüth, A new thin-film Pb microsensor based on chalcogenide glasses, *Sensors and Actuators B*, 71(1-2) (2000) 13–18.
- [24] M. Kassem, D. Le Coq, M. Bokova, E. Bychkov, Chemical and structural origin of conductivity changes in CdSe–AgI–As<sub>2</sub>Se<sub>3</sub> glasses, *Solid State Ionics*, 181 (2010) 466–472.
- [25] M. Kassem, D. Le Coq, M. Fourmentin, F. Hindle, M. Bokova, A. Cuisset, P. Masselin, E. Bychkov, Synthesis and properties of new CdSe–AgI–As<sub>2</sub>Se<sub>3</sub> chalcogenide glasses, *Materials Research Bulletin*, 46 (2011) 210–215.
- [26] M. Kassem, D. Le Coq, R. Boidin, E. Bychkov, New chalcogenide glasses in the CdTe–AgI–As<sub>2</sub>Te<sub>3</sub> system, *Materials Research Bulletin*, 47 (2012) 193–198.
- [27] M. Kassem, S. Khaoulani, A. Cuisset, D. Le Coq, P. Masselin, E. Bychkov, Mercury thioarsenate glasses: a hybrid chain/pyramidal network, *RSC Adv.*, 4 (2014) 49236.
- [28] S. Khaoulani, M. Kassem, S. Fourmentin, E. Bychkov, The AgI–HgS–As<sub>2</sub>S<sub>3</sub> glassy system: Macroscopic properties and Raman scattering studies, *Journal of Alloys and Compounds*, 685 (2016) 752–760.

- [29] CRC Handbook of Chemistry and Physics, 78th edition. In: Lide DR, editor. New York, CRC Press, 1998.
- [30] D. J. E. Mullen, W. Nowacki, Refinement of the crystal structures of realgar, AsS and orpiment,  $As_2S_3$ , *Zeitschrift für Kristallographie*, 136 (1972) 48–65.
- [31] A.M. Al-Syadi, M.S. Al-Assiri, Hassan M.A. Hassan, Gaber El Enany, M.M. El-Desoky, Effect of sulfur addition on the electrochemical performance of lithium-vanadium-phosphate glasses as electrodes for energy storage devices, *Journal of Electroanalytical Chemistry*, 804 (2017) 36-41
- [32] K. L. Bhatia, S. C. Katyal, A. K. Sharma, On the glass formation tendency in  $(PbS)_x \cdot (M_2S_3)_{1-x}$  ( $M = As, Sb$ ), *J. Non-Cryst. Solids*, 58(1) (1983) 27–34.
- [33] Z. U. Borisova, E. A. Bychkov and Y. S. Tveryanovich, *Interaction of Metals with Chalcogenide Glasses*, St. Petersburg University Press, St. Petersburg, 1991.
- [34] M. Kassem, S. Khaoulani, E. Bychkov, Ionic transport in AgI-HgS- $As_2S_3$  glasses: Critical percolation and modifier-controlled domains, *Journal of American Ceramic Society*, 101 (2018) 2287–2296.
- [35] E. Bychkov, Superionic and ion-conducting chalcogenide glasses: Transport regimes and structural features, *Solid State Ionics*, 180 (2009) 510–516.
- [36] E. Bychkov, A. Bychkov, A. Pradel, and M. Ribes, Percolation transition in Ag-doped chalcogenide glasses: comparison of classical percolation and dynamic structure models, *Solid State Ionics*, 113–115 (1998) 691–695.
- [37] E. Bychkov, D. L. Price, C. J. Benmore, and A. C. Hannon, Ion transport regimes in chalcogenide and chalcohalide glasses: from the host to the cation-related network connectivity, *Solid State Ionics*, 154–155 (2002) 349–359.
- [38] V. Vassilev, K. Tomova, S. Boycheva, Pb(II)-ion-selective electrodes based on chalcogenide glasses, *J. Non-Cryst. Solids*, 353(29) (2007) 2779–2784.

- [39] Yu. G. Vlasov, E. A. Bychkov, Electrochemical ion-selective sensors based on chalcogenide glasses, *Sensors and Actuators*, 12 (1987) 275-283.
- [40] E. Bychkov, Spectroscopic studies of chalcogenide glass membranes of chemical sensors: local structure and ionic response, *Sensors and Actuators B*, 26-27 (1995) 351-359.
- [41] M. Miloshova, E. Bychkov, V. Tsegelnik, V. Strykanov, H. Klewe-Nebenius, M. Bruns, W. Hoffmann, P. Papet, J. Sarradin, A. Pradel, M. Ribes, Tracer and surface spectroscopy studies of sensitivity mechanism of mercury ion chalcogenide glass sensors, *Sensors and Actuators B*, 57 (1999) 171-178.
- [42] G. Eisenman, The origin of the glass electrode potential, in: G. Eisenman (Ed.), *Glass Electrodes for Hydrogen and Other Cations. Principles and Practice*, Marcel Dekker, New York, 1967, pp. 133-173.
- [43] B.P. Nicolsky, Theory of the glass electrode, *J. Phys. Chim.*, 10 (1937) 495-503.
- [44] M. Miloshova, D. Baltes, E. Bychkov, New chalcogenide glass chemical sensors for S<sub>2</sub><sup>-</sup> and dissolved H<sub>2</sub>S monitoring, *Water Science Technology*, 47(2) (2012) 135-140.
- [45] M. Milochova, M. Kassem, E. Bychkov, Chalcogenide Glass Chemical Sensor for Cadmium Detection in Industrial Environment, *ECS Transactions*, 50(12) (2012) 357-362.



x1,000 V acc=15.0kV 10 $\mu\text{m}$  LPCA 4/2/2021  
Mode=SEM FOV=120 $\mu\text{m}$ x90 $\mu\text{m}$

